

# Effects of O, H and N passivation on photoluminescence from porous silicon

Z.H. Xiong\*, L.S. Liao, S. Yuan, Z.R. Yang, X.M. Ding, X.Y. Hou

*Surface Physics Laboratory, National Key Laboratory, Fudan University, Shanghai 200433, PR China*

Received 15 January 2000; received in revised form 2 November 2000; accepted 8 November 2000

## Abstract

A simple but effective passivation method for porous silicon (PS) has been developed. Immersion of as-etched PS in dilute  $(\text{NH}_4)_2\text{S}/\text{C}_2\text{H}_5\text{OH}$  solution followed by ultraviolet light irradiation in air can lead to an enhancement of photoluminescence (PL) up to more than 20 times. Infrared absorption and Auger electron spectroscopic measurements show that the formation of  $\text{SiH}(\text{O}_3)$ ,  $\text{Si-O-Si}$  and  $\text{Si-N}$  bonds are formed during the post-treatment process. However, the PL intensity cannot be enhanced if the solution-treated sample is exposed to the laser beam in vacuum. It is thus concluded, that the PL enhancement can be attributed to the presence of compact passivation films consisting of the oxides and the nitride on both external and internal surfaces of the sponge-like PS samples. © 2001 Elsevier Science B.V. All rights reserved.

PACS: 78.55.Mb; 81.65.Rv; 78.30.Ly

Keywords: Porous silicon; Luminescence; Infrared spectroscopy; Auger electron spectroscopy

## 1. Introduction

Since the discovery of room-temperature (RT) visible light emission from porous silicon (PS) in 1990 [1], tremendous efforts have been made to study the photoluminescence (PL) and electroluminescence (EL) from PS-based devices in hopes of optoelectronic integration. At the end of 1996, Hirschman et al. [2] succeeded in integrating PS optoelectronic devices into standard Si-based microelectronics circuits, preliminarily realizing all Si-based optoelectronic integration in a prototype. This progress was encouraging, yet problems concerning the long-term operation of the devices remained to be solved. It has been generally recognized that the visible light emission from high porosity PS is not stable in ambient air, especially under illumination of ultraviolet (UV) light. To stabilize the luminescent

behavior of a PS device, appropriate post-treatment [3,4] is required to effectively passivate the internal surface of the PS. The basic idea of passivation is to replace relatively easy-broken Si-H bonds, which are formed during the hydro-fluoride (HF) anodic etching, by a compact  $\text{SiO}_x$  or Si-N bonds on the surface of PS particles. In previous work [5–7], some post-treatment methods were employed to passivate PS and PL emission from the treated samples was improved to a certain extent. In this work, we report a heating- or plasma-assistance-free passivation technique that PS is simply immersed in  $(\text{NH}_4)_2\text{S}/\text{C}_2\text{H}_5\text{OH}$  solution and then irradiated by UV light in air. The PL from the PS samples so treated is enhanced by a factor up to more than 20 times with an improved stability.

## 2. Experimental

The silicon substrates used were (100) oriented, p-type wafers with the resistivity of 20  $\Omega$  cm. The PS

\* Corresponding author. Tel.: +86-21-65642683; Fax: +86-21-65104949.

E-mail address: zhixiong@fudan.edu (Z.H. Xiong).

samples were prepared by anodizing the wafer in HF solution (50% HF/C<sub>2</sub>H<sub>5</sub>OH = 1:1) at a current density of 10 mA/cm<sup>2</sup> for 5 min. After being cleaned by deionized water and dried by blowing N<sub>2</sub> over the wafers, the samples showed a red color under UV light illumination. The post-treatment process consisted of two steps. (i) The as-etched PS samples were immersed into a C<sub>2</sub>H<sub>5</sub>OH-dilute (NH<sub>4</sub>)<sub>2</sub>S solution [(NH<sub>4</sub>)<sub>2</sub>S/C<sub>2</sub>H<sub>5</sub>OH = 1:200] at RT for 30, 60, 90, 120, 150 and 180 s, respectively. It was observed that a large amount of tiny gas bulbs emerged from the PS surface during the chemical treatment. After immersion, the samples were cleaned by deionized water and blown dry by N<sub>2</sub>. (ii) The immersed samples were exposed to an UV lamp with wavelength of 365 nm. Compared with the as-etched PS, luminescence from the treated samples was strong at the beginning, further intensified in several minutes and ultimately reached a maximum and stabilized after irradiation with the UV light for approximately 2 h.

The samples were characterized by PL, temperature dependence of PL, Auger electron spectroscopy (AES) and Fourier transform infrared (FTIR) measurement. The PL spectra were excited at RT either in air or in vacuum by a 441.6-nm He–Cd laser with a spot size of ~1 mm at a power of 40 mW. The temperature dependence of PL was performed in a rapid-thermal-annealing furnace with the heating rate of 40–50°C/s under the N<sub>2</sub> flow of 6 l/min. The AES measurements were carried out by a PHI 550-electron spectrometer with a primary electron beam energy of 3 keV. The FTIR spectra were measured in a wavenumber range of 400–4600 cm<sup>-1</sup> by an FTIR 5DX spectrometer with a resolution of 4 cm<sup>-1</sup>.

### 3. Results

#### 3.1. PL spectra

Fig. 1 shows the PL spectra of the as-etched sample (a) and the treated samples (b–g) subjected to immersing time for 30, 60, 90, 120, 150 and 180 s, respectively, followed by exposure to the 365-nm UV light for 2 h in air. Comparing curves (b–g) with (a), it can be seen that both intensities and peak positions are changed for the treated samples. The enhancement in the PL intensity can be as high as more than 20 times and the peak position is 20 nm blue-shifted. For the as-etched PS sample in this work, the optimal immersing time was 120 s (i.e. curve (e) in Fig. 1) under the condition of a fixed content (1:200) of the (NH<sub>4</sub>)<sub>2</sub>S/C<sub>2</sub>H<sub>5</sub>OH solution. In addition, for another as-etched larger porosity sample with higher PL intensity (anodized with a higher current density of 50 mA/cm<sup>2</sup> for 5 min), a similar PL enhancement is also observed by adopting an appropriate solution concentration or immersing time. There-

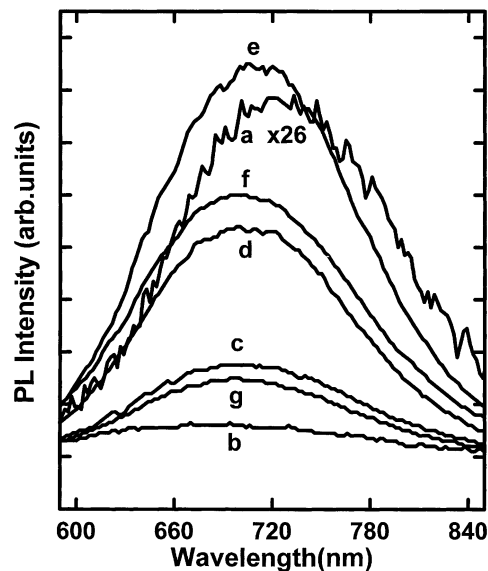


Fig. 1. PL spectra of an as-etched sample (a) and the samples immersed in the (NH<sub>4</sub>)<sub>2</sub>S solution for 30 (b), 60 (c), 90 (d), 120 (e), 150 (f) and 180 s (g), respectively, followed by UV light irradiation for 2 h in air.

fore, these experimental results have shown that the proposed post-treatment method is straightforward and effective in the enhancement of PL from PS.

Moreover, in a series of trial experiments, the significant decays of PL intensity from the treated samples were observed when the concentrate of (NH<sub>4</sub>)<sub>2</sub>S solution in the solution was much higher than 1:200. It implied that (NH<sub>4</sub>)<sub>2</sub>S had a dominant influence on the PL characteristics of the treated samples and C<sub>2</sub>H<sub>5</sub>OH in the solution was only for dilution.

#### 3.2. FTIR spectra

Curve (a), (b) and (c) in Fig. 2 show the FTIR spectra measured from samples of: (1) as-etched PS; (2) 120 s immersion in the 1/200 (NH<sub>4</sub>)<sub>2</sub>S solution; and (3) 120 s immersion followed by 2-h UV irradiation, respectively. The absorption peaks are essentially related with Si–Si (at 619 cm<sup>-1</sup>) and Si–H bonds [8] for sample (1). They are the deformation mode of SiH (665 cm<sup>-1</sup>) [8], the scissors mode of SiH<sub>2</sub> (906 cm<sup>-1</sup>) [9], the stretching modes of SiH (2090.6 cm<sup>-1</sup>) and SiH<sub>2</sub> (2116.4 cm<sup>-1</sup>) [10] and another stretching mode of SiH<sub>3</sub> (a shoulder at 2140 cm<sup>-1</sup>). The absorption peak at 1105 cm<sup>-1</sup> can be ascribed to Si–O stretching, which is relatively weak in curve (a).

The (NH<sub>4</sub>)<sub>2</sub>S immersion results in significant changes of the spectrum. Accompanying intensity reduction of the Si–Si and Si–H related peaks, some new peaks emerge in curve (b). Table 1 lists the variations observed along with assignments of the new peaks [11–17]. The symbols \*, † and ‡, in the first column represent the

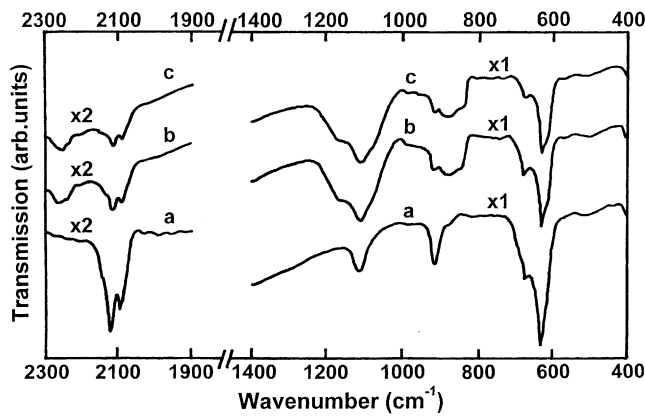


Fig. 2. FTIR spectra of the PS samples of: (1) the as-etched PS; (2) PS immersed in the  $(\text{NH}_4)_2\text{S}$  solution for 120 s; and (3) PS immersed in the  $(\text{NH}_4)_2\text{S}$  solution for 120 s followed by UV light irradiation for 2 h in air.

newly-produced, increased- and decreased-intensity peaks, respectively, and no symbol means little significant change in comparison with curve (a). Emergence of the peaks at 878.12 and 2258.2  $\text{cm}^{-1}$  is an evidence of the formation of  $\text{HSi}(\text{O}_3)$  (back-bond oxidation of Si–H). The strong absorption feature in the wavenumber range of 980–1250  $\text{cm}^{-1}$  originates surely from asymmetric stretching of Si–O–Si and can be attributed to oxidation of PS. The 837.69  $\text{cm}^{-1}$  peak results from the formation of Si–N bonds. Some physisorbed states of nitrogen ( $\text{NH}_3$  or  $\text{NH}_4^+$ ) could be ruled out because their adsorptions (peaked in the regions 3200 and 1500  $\text{cm}^{-1}$ ) are not produced here. It is thus concluded, PS is passivated not only by the oxides [ $\text{HSi}(\text{O}_3)$  and Si–O–Si] but also by the nitride (Si–N bonds) upon immersion in the  $(\text{NH}_4)_2\text{S}/\text{C}_2\text{H}_5\text{OH}$  solution.

Exposure of the  $(\text{NH}_4)_2\text{S}$ -immersed sample to the UV light leads to an overall enhancement of the PL intensity. In order to find out the changes of chemical bonds on the surface of sample (2) after the UV illumination, the FTIR spectrum of sample (3) [sample (2) subjected to 2-h UV irradiation in air] is measured

and shown by curve (c) in Fig. 2. Comparing curve (c) with (b), one can see that a shoulder appears at the lower energy side of the Si–Si ( $619 \text{ cm}^{-1}$ ) peak and the intensities of the oxygen-related peaks get slightly higher while the Si–H<sub>x</sub> peaks become weaker. This indicates that, after the UV irradiation in air, the  $(\text{NH}_4)_2\text{S}$ -immersed sample is further oxidized and the enhanced PL results from the improved quality of the passivation film [18].

### 3.3. AES spectra

The existence of oxygen- and nitrogen-containing compounds on the treated sample surface has been further confirmed by AES measurements. Fig. 3 shows AES depth profile of the  $(\text{NH}_4)_2\text{S}$ -immersed and UV-irradiated sample [sample (3)]. Curves (a), (b), (c) and (d) in the figure correspond to the concentration distributions of Si, O, N and S (C and F ignored) with the  $\text{Ar}^+$  sputtering time, respectively. Comparing from the curve (a), (b), (c) and (d), the content of Si, O, N and S in the treated sample surface is approximately 65, 25, 8 and 2%, respectively, which means that the compounds [ $\text{HSi}(\text{O}_3)$ , Si–O–Si, nitride shown in FTIR] containing O, N and less S are formed after the post-treatment. It can be clearly seen that, while the content of nitrogen decreases steadily till its complete disappearance after approximately 3-min sputtering, the oxygen signal does not disappear ultimately, though it reduces rapidly at the beginning. Obviously, the after-treatment in the  $(\text{NH}_4)_2\text{S}/\text{C}_2\text{H}_5\text{OH}$  solution promotes oxidation of the surface, probably due to the presence of the  $\text{S}^{2-}$  and/or  $\text{HS}^-$  ions, which may catalyze the reaction in the solution. It is also noticeable that the nominal thickness of the passivation film is far beyond monolayer region as 3-min sputtering may remove a much thicker overlayer. In the case of S-passivation of GaAs [19], where the surface GaS film was produced by direct reaction between  $(\text{NH}_4)_2\text{S}$  and bulk GaAs, the passivation layer was much thinner (one monolayer approx.). This can be ascribed to the structural difference of the

Table 1

The oscillation frequencies of the PS immersed in the solution  $(\text{NH}_4)_2\text{S}/\text{C}_2\text{H}_5\text{OH}$  for 120 s [sample (2)]

Absorption peak ( $\text{cm}^{-1}$ )	Bond groups	Oscillation mode	Reference
↓ 619	Si–Si		[8]
665.43	$\text{SiH}_n$	Deformation	[8]
* 837.69	Si–N	Stretching	[11–13] [14,15]
* 878.12	$\text{HSi}(\text{O}_3)$	Bending	[13,16]
↓ 906.25	$\text{SiH}_2$	Scissors	[10]
↑ 1104.9	Si–O–Si	Stretching	[17]
* 1157.6	Si–O–Si	Stretching	[17]
↓ 2090.6	$\text{SiH}_2$	Stretching	[9]
↓ 2116.4	SiH	Stretching	[9]
* 2258.2	$\text{HSi}(\text{O}_3)$	Stretching	[13,16]

two systems: the sponge-like PS sample has a much higher surface-to-volume ratio; and both of its external and internal surfaces can be terminated by foreign atoms. Further prolonging  $\text{Ar}^+$  etching time, the content of O is originated from the oxide passivation films on the internal surface of the treated PS. Therefore, we regard the enhanced PL intensity shown in Fig. 1 as a result of termination of both the external and internal surfaces of the sponge-like PS by  $\text{HSi}(\text{O}_3)$ ,  $\text{Si-O-Si}$  and  $\text{Si-N}$  bonds.

### 3.4. PL vs. the laser exposure time

In order to study the influence of laser illumination on PL, the continuous change of PL from sample (2) vs. the illumination time has been measured and the results are shown in Fig. 4. No discernible peak shift could be observed when discrete PL spectra were measured, indicating that the integrated intensity and the individual peak intensity had the same time dependence. Curve (a) was measured in the atmosphere. To detect the oxygen influence on the PL from sample (2) when illuminated under laser light, its PL was also measured in vacuum ( $\sim 10^{-3}$  torr) and is shown by curve (b). The two curves show a rapid decay at the very beginning of illumination. Completely different behaviors are then observed in the two cases. In case (a) (measured in air), the PL intensity rises steadily and finally saturates at a value much higher than initially reached, but in case (b), the PL intensity decreases monotonically and finally reaches a very low value. Moreover, the PL intensity does not decrease but slightly increases on the base of the stabilized value when the same tested spot on the sample (2) is measured again after 2 h, as shown in curve (a). This demonstrates that the enhanced PL is not the result of

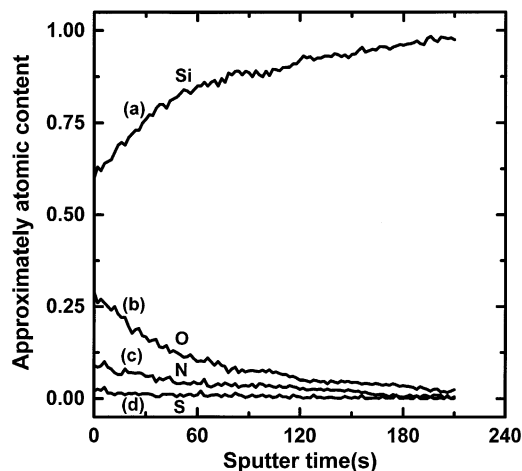


Fig. 3. AES depth profile of sample (3), (PS immersed in the  $(\text{NH}_4)_2\text{S}$  solution for 120 s followed by UV light irradiation for 2 h in air). (a), (b), (c) and (d) are for concentration distribution of Si, O, N and S, respectively.

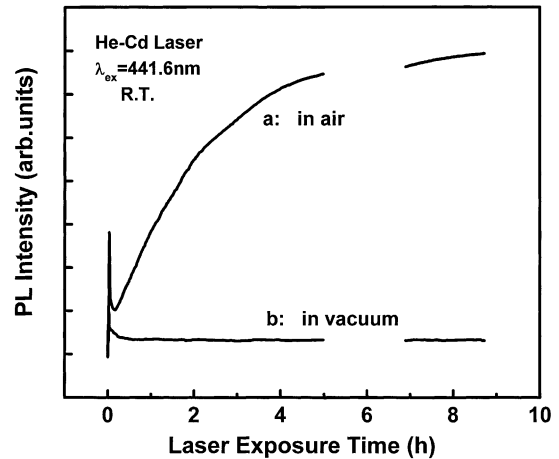


Fig. 4. Evolution of PL intensity (peaked at 700 nm) vs. the laser illumination time from sample (2) (immersed in the  $(\text{NH}_4)_2\text{S}$  solution for 120 s) measured in air (a) and in the vacuum ( $\sim 10^{-3}$  torr) (b), respectively.

the heat effect due to the long-time illumination of laser light and is stable when it saturates. Comparing curve (a) with (b), the PL enhancement measured in the vacuum is not observed, which indicates the dependence of PL enhancement on oxygen in the atmosphere, that is, a process of oxidation induced by light (including laser beam and ultraviolet light). The decrease of PL from the as-etched PS sample (1) was observed upon illumination with a laser beam in air, so the enhancement of PL from sample (3) should be closely relative to the proposed post-treatment. From the curve (b) and (c) in Fig. 2, the absorption peaks relative with oxygen become slightly higher when sample (2) is exposed under the UV light. This shows that the quality of the passivation film [for example,  $\text{HSi}(\text{O})_3$ ,  $\text{Si-O-Si}$ ] is improved by the light illumination. We speculate that UV or laser beam irradiation in air after the  $(\text{NH}_4)_2\text{S}$  immersion stimulates further oxidation of the passivation layer and a higher compactness is then achieved. In addition, the structure of passivation film becomes more stable with longer exposure time until the PL intensity has reached a maximum value.

### 3.5. PL vs. the rapid thermal annealing temperature

Fig. 5 shows the dependence of the integrated intensity [curve (a)] and the peak wavelength [curve (b)] of PL from sample (3) vs. the temperature of the rapid thermal annealing in  $\text{N}_2$  gas, respectively. All the tested samples are cut from a same sample. The results shown in curve (b) are somewhat the same as that of rapid thermal oxidation (RTO) method [5]. That is, the peak shifts little below  $500^\circ\text{C}$ , while there is an obvious blue-shift above  $500^\circ\text{C}$ . Nevertheless, from curve (a), when the temperature rises from RT to  $600^\circ\text{C}$ , the intensity first increases and then reaches a maximum at

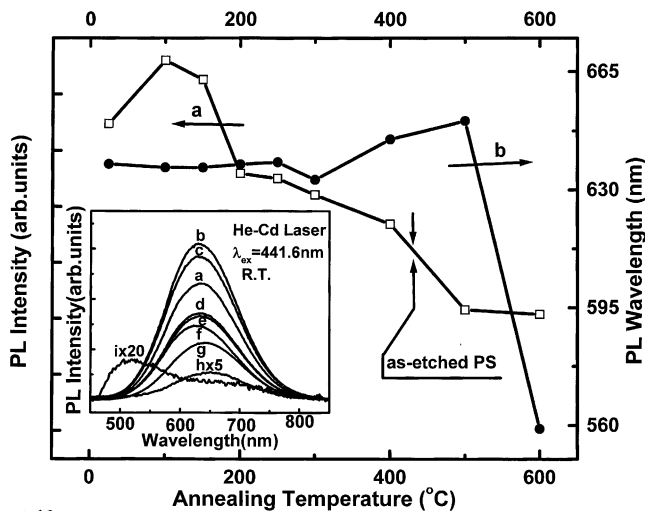


Fig. 5. Temperature dependence of PL from sample (3) (immersed in the solution  $(\text{NH}_4)_2\text{S}$  for 120 s followed by UV light irradiation for 2 h in air). Curve (a) and (b) represent the PL intensities and peak wavelengths vs. the temperature of the rapid thermal annealing in  $\text{N}_2$  gas, respectively. The inset illustrates the discrete PL spectra of the treated sample (3) subjected to the rapid thermal annealing temperature of RT (a), 100 (b), 150 (c), 200 (d), 250 (e), 300 (f), 400 (g), 500 (h) and 600°C (i), respectively.

100°C and gradually decays till it disappears, which is different from the results of RTO. The RTO temperature at the peak of integrated intensity is 900°C, however, the temperature for our experiment is approximately 100°C. In addition, as shown in curve (a), the PL intensity from sample (3) is higher than that of the as-etched sample (1) at RT, although the sample (3) is heated to 400°C. So, the proposed post-treatment method could also be effective for the future potential application in PS device development.

#### 4. Discussion

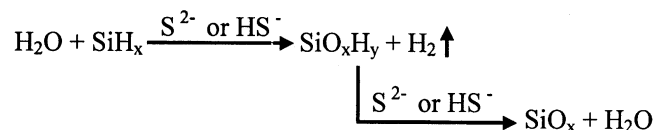
Although hydrogen can effectively saturate dangling bonds and hence contribute to the formation of a stable passivation film  $\text{SiH}_x$  on flat surfaces of crystalline Si [20].  $\text{SiH}_x$  is not stable on the pore surface of as-etched PS, where H is easily desorbed or oxidized, leading to the creation of a large amount of non-radiation recombination centers and an unstable PL. Therefore, it is highly desired to find more effective passivation methods. For microelectronic application, the oxides or nitrides of Si (for example,  $\text{SiO}_x$  and  $\text{Si-N}$ ) have been currently considered as the most practical passivation films. As we know, there are several results of the oxidation influence on PL from PS: one causes non-radiation recombination centers on the pore surface of porous Si grains that results in the reduced and unstabilized PL [21–23], the other leads to enhanced PL [7,18,24]; and in another case, initially PL decays, then it increases and finally decreases again [5]. These

results are directly relative with the PS formation processes and the post-treatment methods of PS. Demonstrated by Chen et al. [24], who had achieved the enhanced PL from a PS post-treated with wet thermal oxidation method,  $\text{HSi}(\text{O}_3)$  is stable under the laser illumination. This is due to the back-bond oxidation of Si–H, the interatomic distance between Si and H becomes shorter and the interatomic force between them becomes stronger in comparison with that of the SiH bonds on the surface of an as-etched PS. From the FTIR spectra shown in Fig. 2, the absorption peaks of  $\text{HSi}(\text{O}_3)$  (at 2258.2 and 878.12  $\text{cm}^{-1}$ ) and Si–O–Si (ranged from 980 to 1250  $\text{cm}^{-1}$ ) are similar to that of the PS treated by the oxygen incorporation method with utilizing the remote-plasma treatment proposed by Xiao et al. [7], who attained the enhanced PL from the post-treated PS, too. Therefore, as mentioned above, the passivation films of  $\text{HSi}(\text{O}_3)$  and Si–O–Si could enhance the intensity and stability of PL from the as-etched PS. The dangling bonds density on the surface of the PS treated by RTN [6] with  $\text{SiN}_x$  are very low so as to stabilize the PL. Therefore  $\text{SiN}_x$  is a good passivation film not only for bulk crystal Si but also PS. Based on the FTIR shown in Fig. 2, the  $\text{HSi}(\text{O}_3)$ , Si–O–Si and Si–N bonds have grown on the surface of PS treated by the proposed method. So, the enhancement of PL from the treated sample should be the results of the ensemble actions of the several passivation films.

The absorption peaks relative to sulfur is seldom found on the surface of the treated sample from the FTIR spectra shown in Fig. 2. Meanwhile, there were many absorption peaks relative with oxygen (e.g.  $\text{HSi}(\text{O}_3)$  and Si–O–Si), whose intensities are much higher than others. Based on this fact, we assume that the ions  $\text{S}^{2-}$  or  $\text{HS}^-$  in the  $(\text{NH}_4)_2\text{S}$  solution act as a catalyst for the oxidation reaction: for the formation of  $\text{HSi}(\text{O}_3)$  and Si–O–Si passivation film. A similar result could be concluded from the concentration distribution of O and S in the AES measurement illustrated in Fig. 4.

#### 5. Conclusion

We have reported the enhancement of the PL intensity and stability due to the formation of the passivation film of  $\text{HSi}(\text{O}_3)$ , Si–O–Si and Si–N on the surface of PS immersed in the solution  $(\text{NH}_4)_2\text{S}/\text{C}_2\text{H}_5\text{OH}$  and then illuminated under UV light. The PL intensities from the treated PS are several to more than 20



times higher than that of the as-etched PS. Moreover, the PL is quite stable even illuminated by laser beam for several hours. Therefore, the proposed method could be considered as a straightforward and effective technique for achieving intense and stable light emission from porous silicon.

### Acknowledgements

The authors would like to thank X.A. Cao for his helpful discussions. This work is partially supported by the National Science Foundation of China with Grant No. 59832100.

### References

- [1] L.T. Canham, *Appl. Phys. Lett.* 57 (1990) 1046.
- [2] K.D. Hirschman, L. Tsyhckov, S.P. Duttagupta, P.M. Fauchet, *Nature* 384 (1996) 338.
- [3] M.A. Tischler, R.T. Collins, J.H. Stathis, J.C. Tsang, *Appl. Phys. Lett.* 60 (1992) 639.
- [4] R.T. Collins, M.A. Tischler, J.H. Stathis, *Appl. Phys. Lett.* 61 (1992) 1649.
- [5] V. Petrova-Koch, T. Muschik, A. Kux, B.K. Meyer, F. Koch, V. Lehmann, *Appl. Phys. Lett.* 61 (1992) 943.
- [6] G.B. Li, X.Y. Hou, S. Yuan, H.J. Chen, F.L. Zhang, H.L. Fan, X. Wang, *J. Appl. Phys.* 80 (1996) 5967.
- [7] Y. Xiao, M.J. Heben, J.M. McCullough, Y.S. Tsuo, J.L. Pankove, S.K. Deb, *Appl. Phys. Lett.* 62 (1993) 1152.
- [8] P. Gupta, V.L. Colvin, S.M. George, *Phys. Rev.* B37 (1988) 8234.
- [9] H. Wagner, R. Butz, U. Backs, D. Burchmann, *Solid State Commun.* 38 (1981) 1155.
- [10] A. Venkateswara Rao, F. Ozanam, J.N. Chazalviel, *J. Electrochem. Soc.* 138 (1993) 153.
- [11] G. Lucovsky, J. Yang, S.S. Chao, J.E. Tyler, W. Czubytyj, *Phys. Rev.* B28 (1983) 3234.
- [12] W. Ewing, *Instrumental Method of Chemistry Analysis*, 5th edition, McGraw-Hill Press, New York, 1985, p. 95.
- [13] G. Lucovsky, J. Yang, S.S. Chao, J.E. Tyler, W. Czubytyj, *Phys. Rev.* B28 (1983) 3225.
- [14] D.V. Tsu, G. Lucovsky, *J. Vac. Sci. Technol.* A4 (1986) 480.
- [15] G. Lucovsky, P.D. Richard, D.V. Tsu, S.Y. Lin, R.J. Markunas, *J. Vac. Sci. Technol.* A4 (1986) 681.
- [16] D.V. Tsu, G. Lucovsky, B.N. Davidson, *Phys. Rev.* B40 (1989) 1795.
- [17] W. Kaiser, P.H. Keck, C.F. Lange, *Phys. Rev.* 101 (1989) 1795.
- [18] S. Shih, K.H. Jung, J. Yan, D.L. Kwong, M. Kovar, J.M. White, T. Geoge, S. Kim, *Appl. Phys. Lett.* 63 (1993) 3306.
- [19] B.A. Cowans, Z. Dardas, M.S. Carperter, M.R. Melloch, *Appl. Phys. Lett.* 54 (1989) 362.
- [20] E. Yublonovitch, D.L. Allare, C.C. Chang, T. Gmitter, T.B. Bright, *Phys. Rev. Lett.* 57 (1985) 249.
- [21] X.L. Zheng, H.C. Chen, W. Wang, *J. Appl. Phys.* 72 (1992) 3841.
- [22] L.T. Canham, M.R. Houlton, W.Y. Leong, C. Pickering, J.M. Keen, *J. Appl. Phys.* 70 (1991) 442.
- [23] D.W. Cooke, B.L. Bennett, E.H. Farnum, W.L. Hults, K.E. Sickafus, J.F. Smith, J.L. Smith, T.N. Taylor, P. Tiwari, *Appl. Phys. Lett.* 68 (1996) 1663.
- [24] H.J. Chen, X.Y. Hou, G.B. Li, F.L. Zhang, M.R. Yu, X. Wang, *J. Appl. Phys.* 79 (1996) 3282.